Appl. Phys. A 79, 1603–1606 (2004)
DOI: 10.1007/s00339-004-2860-2

Applied Physics A
Materials Science & Processing

Z.B. WANG[1,2]
M.H. HONG[1,2,✉]
B.S. LUK`YANCHUK[1]
S.M. HUANG[1]
Q.F. WANG[1,2]
L.P. SHI[1]
T.C. CHONG[1,2]

Parallel nanostructuring of GeSbTe film with particle mask

[1] Data Storage Institute, DSI Building, 5 Engineering Drive 1, Singapore 117608, Republic of Singapore
[2] Department of Electrical and Computer Engineering, National University of Singapore, Singapore 119260, Republic of Singapore

Received: 9 October 2003/Accepted: 26 March 2004
Published online: 26 July 2004 •

ABSTRACT Parallel nanostructuring of a GeSbTe film may significantly improve the recording performance in data storage. In this paper, a method that permits direct and massively parallel nanopatterning of the substrate surface by laser irradiation is investigated. Polystyrene spherical particles were deposited on the surface in a monolayer array by self-assembly. The array was then irradiated with a 248-nm KrF laser. A sub-micron nanodent array can be obtained after single-pulse irradiation. These nanodents change their shapes at different laser energies. The optical near-field distribution around the particles was calculated according to the exact solution of the light-scattering problem. The influence of the presence of the substrate on the optical near field was also studied. The mechanisms for the generation of the nanodent structures are discussed.

PACS 81.16.Mk; 61.80.Ba; 81.16.Rf; 81.65.Cf

1 Introduction

Laser-induced near-field patterning of surfaces at a resolution far below the diffraction limit has attracted more and more attention in recent years due to its extensive potential applications in high-density data storage and high-resolution optical lithography for nanodevice fabrication [1]. In most near-field techniques, the sub-wavelength resolution is achieved by placing a small aperture between the recording medium and the light source. If the aperture-to-medium separation is controlled at a distance much smaller than the wavelength, the resolution will be determined by the aperture size instead of the diffraction limit [2]. This technique is used in the scanning near-field optical microscope (SNOM) system: a single hollow optical fibre with a small aperture at its end is used to deliver the laser beam [3]. Due to the near-field optical enhancement effect at the tip, the SNOM system is able to perform surface modification in a nanoscale of different kinds of materials. However, this approach is difficult to implement in an industrial application due to the need for sophisticated hardware to control the near-field distance and a low throughput. One promising approach that could lead to massively parallel nanostructuring was demonstrated by using a particle mask to pattern a solid substrate [4–6]. The optical near-field enhancement effect is believed to be responsible for the formation of nanostructures under the particles. However, the 'true' field distribution around the particles is still not clear and most of the previous studies mainly use conventional Mie theory to evaluate it, so the substrate effect is neglected. In this paper, we calculate the exact field distribution under a particle and compare the results with those obtained from Mie theory. The influence of the substrate on the near-field distribution is identified. A concept relating to the definition of the near-field intensity is also clarified. The calculated intensity profile is compared with experimental results. The mechanisms for the generation of the nanodent structures on the substrate surface are discussed.

✉ Fax: +65-67771349, E-mail: hong-minghui@dsi.a-star.edu.sg

2 Experimental details

The sample is a 100-nm-thick $Ge_2Sb_2Te_5$ (GST) film coated on a 0.6-mm polycarbonate substrate. The initial state of the as-deposited film is an amorphous phase. The refractive index of the film is about $1.8049 + 2.0657\,\mathrm{i}$. The melting point of the film is 616 °C. Monodisperse polystyrene (PS) particles (Duke Scientific Corp.) with a diameter of 1.0 μm were used. They are transparent to ultraviolet (UV) light. The particle suspension was diluted with deionised (DI) water and deposited on a GST substrate with a dispenser. The sample was then stored inside a refrigerator at 10 °C for 1 h until all the water solvent was evaporated. A KrF excimer laser ($\lambda = 248$ nm, full width at half maximum (FWHM) = 23 ns) was used as a light source. With a single-pulse irradiation, the damage threshold for the GST sample is around 12.0 mJ/cm^2. A lens of 500-mm focal length focused the laser beam onto the sample mounted vertically on a holder. Different laser intensities were used to study the laser-energy dependence of the nanostructures formed on the GST material. The GST surface after laser processing was characterised by a scanning electron microscope (SEM: Hitachi S-4100).

3 Results and discussion

The 1.0-μm non-absorptive spherical PS particles act as microlenses that focus the incident laser radiation onto the substrate [7]. Exact examinations of the near-field intensity distributions, $I \propto EE^* = |E|^2$ or $I = |S_z|$ ($S \propto \mathrm{Re}[EH^*]$), can be done within the framework of classical Mie theory [8].

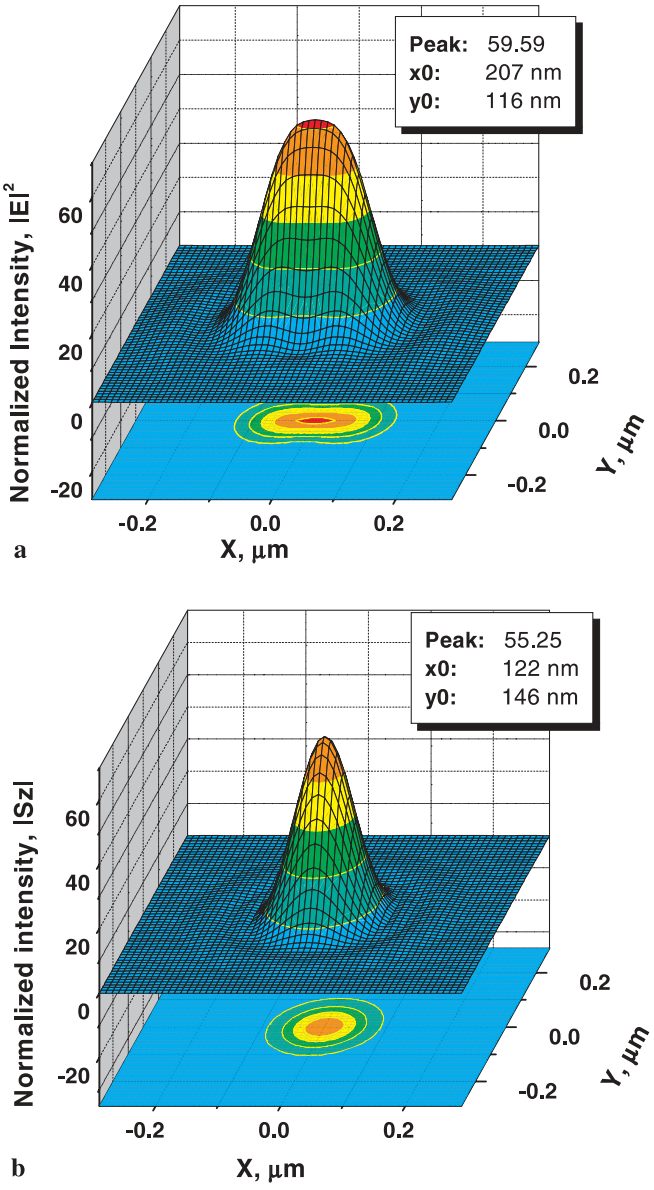

FIGURE 1 Calculated intensity distributions underneath 1.0-µm PS particles from Mie theory. **a** $|E|^2$ intensity and **b** $|Sz|$ intensity. The incident light is x-polarized and propagates along z

Figure 1a and b present the $|E|^2$ intensity distribution and the $|Sz|$ intensity distribution on the surface underneath the particles, respectively, as calculated from rigorous Mie formulae. Although the peak values are close, the intensity profiles are different from each other. The profile of the $|E|^2$ intensity (full width at $1/e$ maximum) is not a round shape but has a ratio of about 2 : 1. However, the $|Sz|$ intensity presents a nearly round focusing. It should be noted that these Mie calculations are only valid for the cases without a substrate present in the light-scattering system. The reflection and secondary scattering of the reflected wave in a particle–substrate system may significantly change the final field distributions around the particles [4, 7]. Numerical simulation for this case is also performed in this study, based on the exact solution in [9]. In order to make a clear comparison, we summarise calculation results in Table 1. The following definitions are used: (1) $X0$: full width at $1/e$ maximum in the x direction (focusing size), (2) $X1$: full width of the region with enhancement effect in the x direction, (3) $Y0$: full width at $1/e$ maximum in the y direction (focusing size), (4) $Y1$: full width of the region with enhancement effect in the x direction, (5) $\Delta d = X0 - Y0$ or $\Delta d = X1 - Y1$.

From Table 1, one can see that the electrical field enhancement at the contact point becomes stronger when the GST substrate is present, increasing from 59.59 to 86.82. Meanwhile, the focusing intensity profile becomes sharper as $X0$ and $Y0$ both decrease ($X0$: 207 nm → 173 nm, $Y0$: 116 nm → 102 nm). The decrease of the Δd value (from 91 nm to 71 nm) indicates that the GST substrate has a 'homogeniser' effect on the electrical field. For the $|S_z|$ field, similar conclusions can be drawn from Table 1. The difference between the $|E|^2$ and $|S_z|$ fields originally comes from the contribution of the r component of the electric vector, E_r, which decays with r as $E_r \propto 1/r^2$. It quickly tends to zero in the optical far field ($r \geqslant \lambda$) [8]. In other words, the scattered wave in the far field is a transverse wave for which the $|E|^2$ and the $|S_z|$ intensities are identical. But the scattered wave in the optical near field is not transverse any more and thus the $|S_z|$ field will differ from the $|E|^2$ field. In principle, one should use the $|S_z|$ intensity field to describe the physical phenomena in the optical near field nanostructuring.

In the experiments, it is found that most of the PS spheres were removed after one laser-pulse irradiation. Consequently, nanodent structures with the same hexagonal pattern were formed on the GST surface at the locations where spheres originally were located. The average diameters of the structures are summarised in Fig. 2. The deviation of the measured diameter is found to be smaller than 40 nm. Comparing this with the Δd value in Table 1, one finds that the $|S_z|$ intensity (Δd: 4–30 nm) fits the result well rather than the $|E|^2$ intensity (Δd: 71–123 nm). From Fig. 2, it can be seen that the diameter of the nanodent increases almost linearly with the laser fluence up to 7.2 mJ/cm^2, but tends to saturate as the laser fluence increases further. The linear increase in the low-fluence region (< 7.2 mJ/cm^2) could be attributed to the enhanced heat-diffusion process as more laser energy is deposited into the substrate when the laser fluence increases. However, when the laser fluence increases further, the particle lens could detach from the substrate in a time interval much smaller than the laser-pulse duration [10]. This effect leads to a saturation tendency of laser energy deposition into

	Peak	$X0/X1$ (nm)	$Y0/Y1$ (nm)	$\Delta d = \lvert X_- - Y_- \rvert$ (nm)
$\lvert E\rvert^2$ (Mie)	59.59	207/328	116/224	91/104
$\lvert E\rvert^2$ (substrate)	86.82	173/305	102/182	71/123
$\lvert S_z\rvert$ (Mie)	55.25	122/210	146/248	24/38
$\lvert S_z\rvert$ (substrate)	72.19	123/228	119/198	4/30

TABLE 1 $|E|^2$ and $|S_z|$ intensity profiles calculated from Mie theory (no substrate) and exact particle-substrate modul

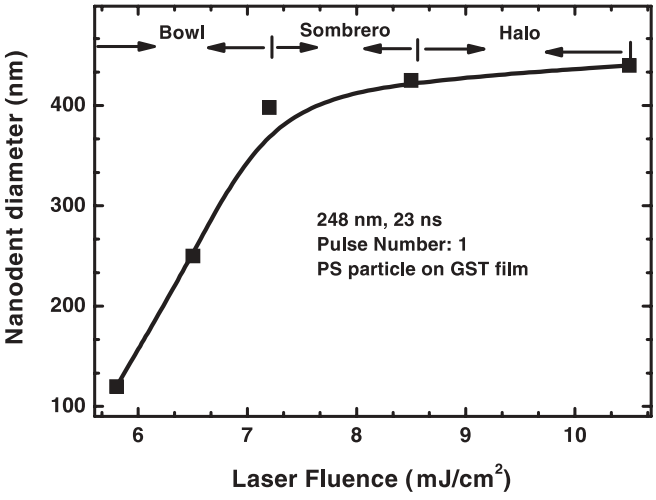

FIGURE 2 Measured mean diameter of the nanodents as a function of laser fluence

the substrate. The total amount of deposited laser energy in such a case is determined by the particle-detachment time instead of the laser-pulse duration. On the other hand, we will see below that the nanodent shape also changes at different laser fluences, indicating the excitation of complex convective fluxes during the melting process. This could also affect the nanodent diameter at different laser fluences. From calculated theoretical values, the saturation size of the nanodent structures is about 200 nm, which is smaller than the experimental value of 400 nm. The deviation is due to the heat-diffusion process in the GST film after laser heating, which transfers the heat energy to surrounding regions. In our experiments, it is observed that damage sites can also be formed on PS particles at a high laser fluence, but with a nanodent diameter around 200 nm. This value is in good agreement with the theoretical value.

Figure 3 shows the SEM images of nanodent structures formed on GST films after one laser pulse irradiation at fluences of 5.8 mJ/cm^2, 8.5 mJ/cm^2 and 10.5 mJ/cm^2, respectively. At the laser fluence of 5.8 mJ/cm^2, bowl-shape dents with a diameter around 120 nm can be observed, as shown in Fig. 3a. The shape of the dents does not change too much for the laser fluence less than 7.2 mJ/cm^2. However, sombrero-shape bumps with an outer rim are formed at a fluence of 8.5 mJ/cm^2, as given in Fig. 3b. When the laser fluence becomes higher, halo-shape dents with an outer ring can be seen in Fig. 3c. Recently, Lu and Chen reported a similar phenomenon for silicon substrates with a native 2-nm-thick SiO_2 layer: bowl-shape dents at low laser fluences and sombrero-shape dents at high laser fluences [11]. However, no halo-shape dents were observed in their work at high laser fluences. The mechanism for the formation of these different nanodent structures is related to the fact that surface melting could result in the excitation of convective fluxes within the liquid layer. Thermocapillary force and chemicapillary force are the two main origins that lead to changes in surface tension [12]. Since the optical field enhancement has a Gaussian-like distribution in our case, the temperature decreases from the centre of the molten zone to its edge. Assuming that the material concentration gradient is small, such a temperature gradient causes an

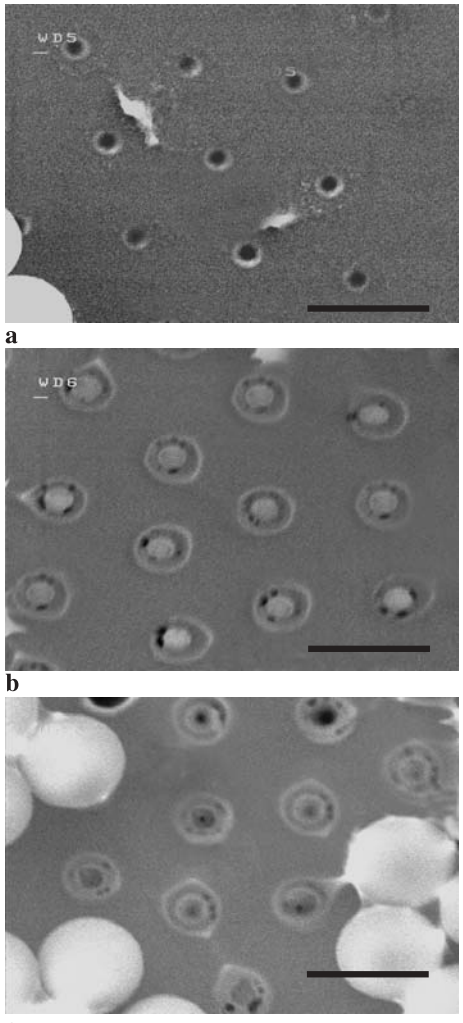

FIGURE 3 SEM images of nanodent structures formed on GST film after one laser pulse irradiation at laser fluences of **a** 5.8 mJ/cm^2, **b** 5.8 mJ/cm^2 and **c** 5.8 mJ/cm^2. Scale bar is 1.0 μm

outward flow of the molten material to the edge. It is believed to be responsible for the formation of the outer rim and the bowl-shape nanodents (Fig. 3a) [11]. When the laser fluence is high enough to trigger the concentration change of the material, convective flow could reverse its direction and a sombrero shape (Fig. 3b) can be observed [11]. However, we are still not clear which composition of GST material changes its concentration and more investigations are needed. When laser fluences become higher, strong evaporation takes place in the central region that generates recoil pressure on the molten material, leading to a halo structure in the centre. At the tail region, the Marangoni convection remains so that an outer ring still exists (Fig. 3c).

4 Conclusions

The difference between the $|E|^2$ and $|Sz|$ fields in the optical near-field problem is investigated. The presence of the substrate influences the final field distributions: (1) the enhancement by the reflection of the substrate is observed near the contacting point and (2) the substrate may help to homogenise the enhancement field. The particle-enhanced

optical near field can be utilised to pattern the GST film in a nanometre scale. By forming a monolayer of a particle array on the substrate by self-assembly, this process can be highly parallel. The formed nanostructures on GST films change their shapes at different laser fluences. Both a Marangoni-driven flow mechanism and an evaporation-driven flow mechanism are involved in the formation of the different structures.

REFERENCES

1 M. Ohtsu, H. Hori: *Near-field Nano-optics* (Kluwer Academic, New York 1999)
2 E. Betzig, J.K. Trautman, R. Wolfe, E.M. Gyorgy, P.L. Finn, M.H. Kryder, C.-H. Change: Appl. Phys. Lett. **61**, 142 (1992)
3 S. Patane, A. Arena, M. Allegrini, L. Amdereozzi, M. Faetti, M. Giordano: Opt. Commun. **210**, 37 (2002)
4 H.-J. Münzer, M. Mosbacher, M. Bertsch, O. Dubbers, F. Burmeister, A. Pack, R. Wannemacher, B.-U. Runge, D. Bäuerle, J. Boneberg, P. Leiderer: Proc. SPIE **4426**, 180 (2001)
5 O. Watanabe, T. Ikawa, M. Hasegawa, M. Tsuchimori, Y. Kawata: Appl. Phys. Lett. **79**, 1366 (2001)
6 K. Piglmayer, R. Denk, D. Bäuerle: Appl. Phys. Lett. **80**, 4693 (2002)
7 B.S. Luk`yanchuk, Y.W. Zheng, Y.F. Lu: Proc. SPIE **4065**, 576 (2000)
8 M. Born, E. Wolf: *Principles of Optics*, 7th edn. (Cambridge University Press, Cambridge 1999)
9 P.A. Bobbert, J. Vlieger: Physica A **137**, 243 (1986)
10 B.S. Luk`yanchuk, N. Arnold, S.M. Huang, Z.B. Wang, M.H. Hong: Appl. Phys. A **77**, 209 (2003)
11 Y. Lu, S.C. Chen: Nanotechnology **14**, 505 (2003)
12 D. Bäuerle: *Laser Processing and Chemistry* (Springer, Singapore 2000)